Supplementary information

Figures

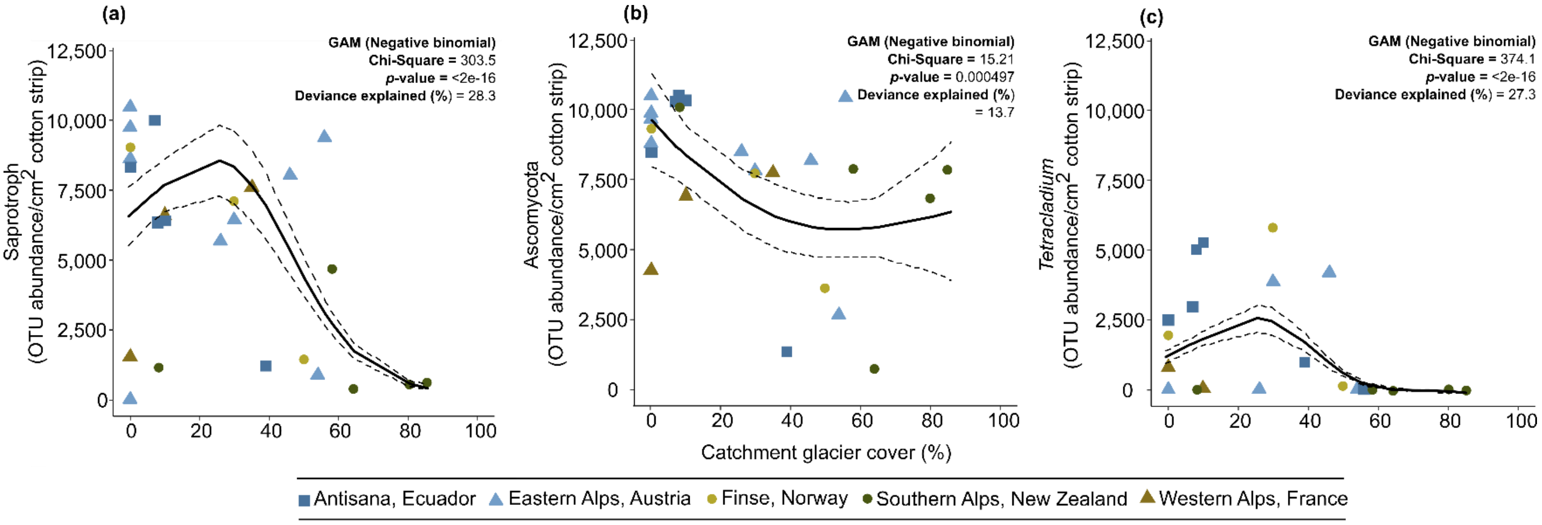

Supplementary Figure 1: Fungal responses to changing catchment glacier cover. The response of subgroups of the fungal community (a - c) identified on cotton-strip assays incubated in glacierised mountain rivers along a gradient of catchment glacier cover. For river sites in the Alaska Boundary Range no amplification was detected. Solid lines are GAMs and dashed lines represent 95% confidence intervals.

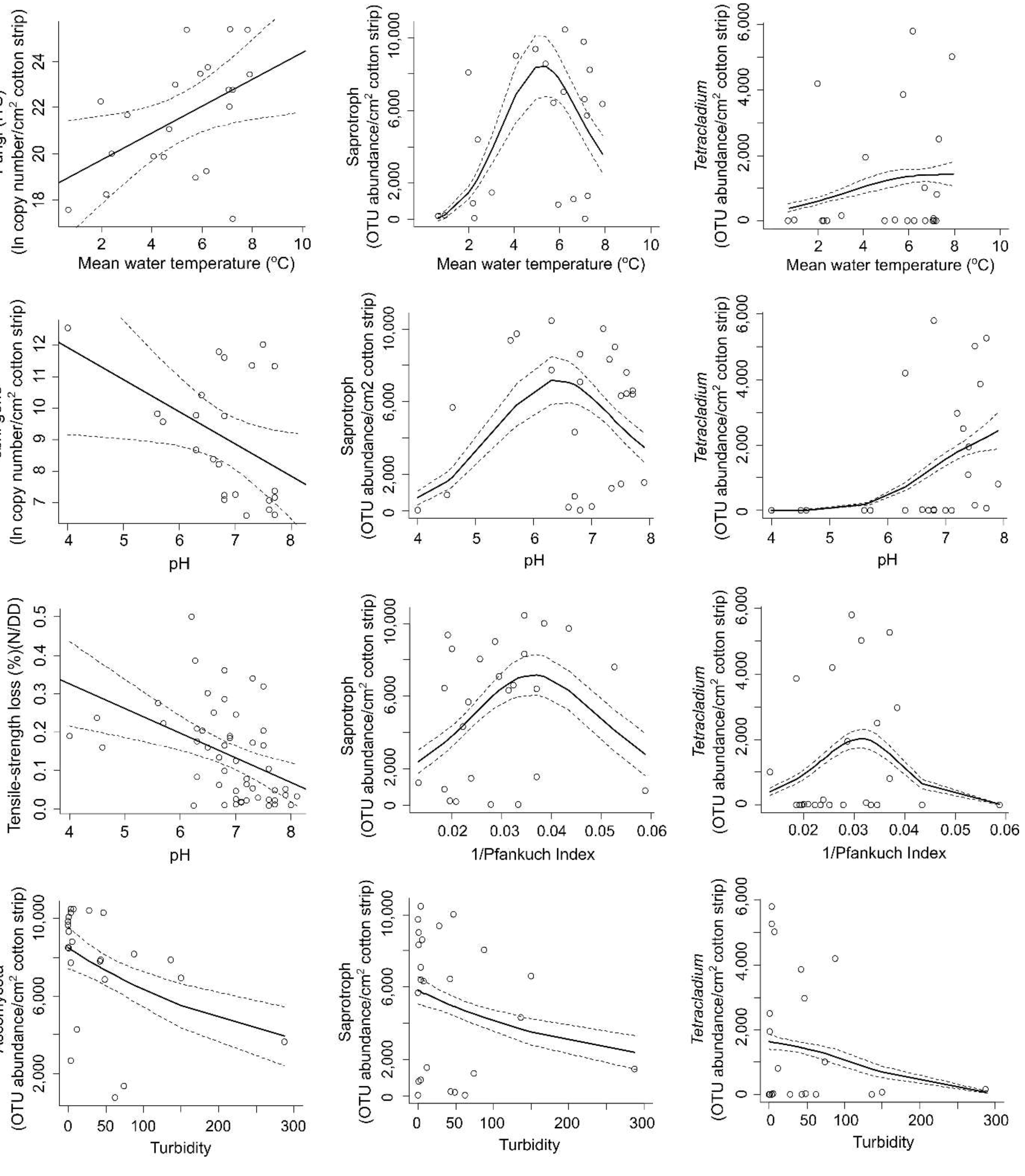

Supplementary Figure 2: Significant GLM/GAM relationships between physicochemical parameters, nutrient concentrations (mg/L) and cotton-strip assay descriptors across six glacierised mountain regions. The fungal community (ITS) is represented as a whole (ln qPCR copy number/cm^2 cotton strip), and as subgroups (Ascomycota, *Tetracladium,* saprotrophs) (OTU abundance/cm^2 cotton strip). The Pfankuch Index is a method for estimating the geomorphic channel stability of rivers[1]. Here, stability of the channel bottom is assessed, and higher scores represent greater stability. Tensile-strength loss (%) (N/DD) pertains to the cotton-strip assay deployed at each river site. Solid lines are GLMs or GAMs and dashed lines represent 95% confidence intervals. Summary statistics are shown in Supplementary Table 2.

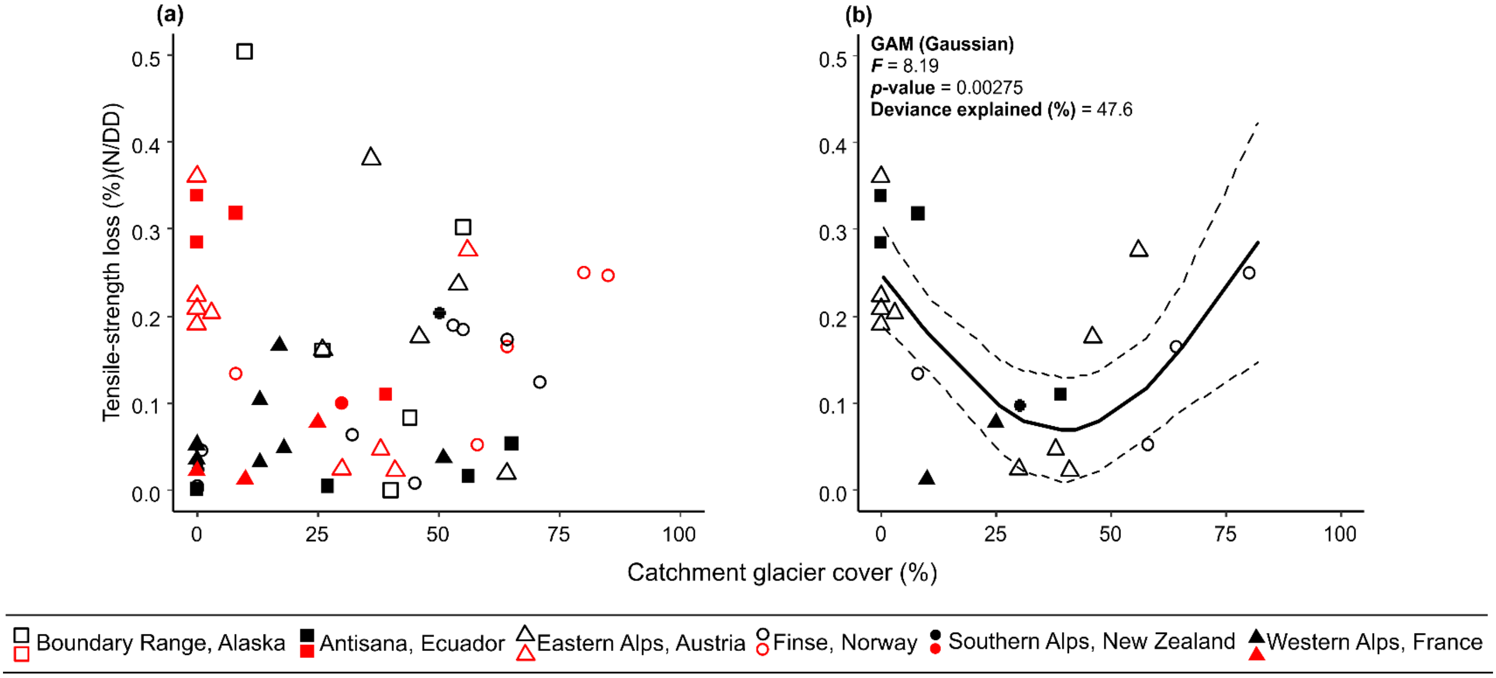

Supplementary Figure 3: Tensile-strength loss values for glacierised mountain rivers spanning a gradient of catchment glacier cover. (a) Mean tensile-strength loss per degree-day and catchment glacier cover of river sites. There was no relationship between tensile-strength loss and catchment glacier cover for all river sites (GAM(Gaussian), $F = 0.92$, $p = 0.404$, deviance explained (%) = 3.5) or those with no fungal ITS/*cbhI* amplification (black symbols: GAM(Gaussian), $F = 0.78$, $p = 0.469$, deviance explained (%) = 6.37). Samples with fungal ITS and/or *cbhI* amplification (red symbols) showed a stronger relationship at $p<0.10$ (GAM(Gaussian), $F = 3.12$, $p = 0.0624$, deviance explained (%) = 20.6). In contrast, (b) mean tensile-strength loss per degree-day and catchment glacier cover for only those river sites hosting *cbhI* amplification was significant at $p<0.05$ (n.b. some but not all of these river sites showed fungal ITS amplification: see Supplementary Table 1).

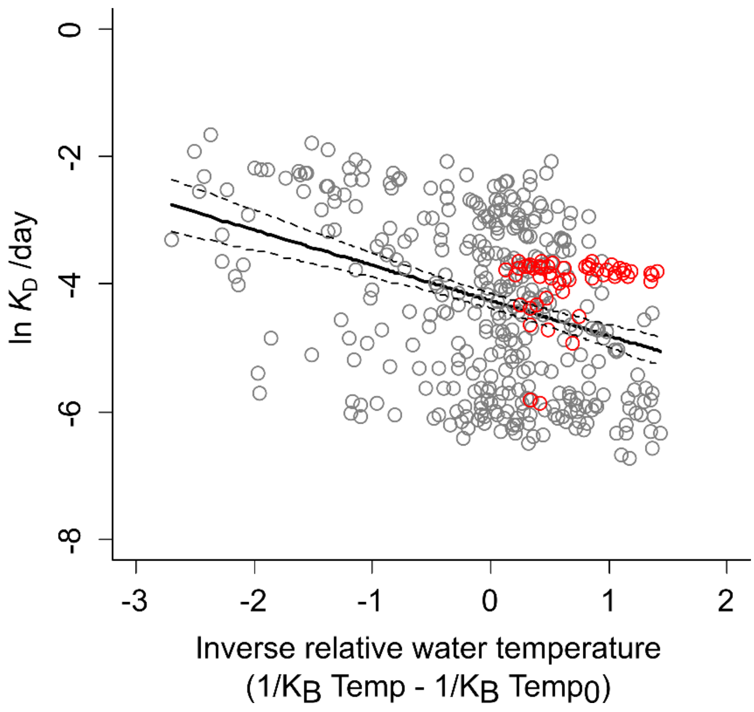

Supplementary Figure 4: Temperature sensitivity of daily cellulose-decomposition rates for rivers in multiple biomes. An Arrhenius plot displaying the relationship between inverse relative river water temperature and non-temperature-adjusted (K_D) daily cellulose-decomposition rates (mean tensile-strength loss per river) for glacierised mountain rivers (○). Equivalent values are also displayed for rivers draining different biomes (○), as recorded by Tiegs et al. (2019)[2], showing that mountain river assays were representative of the global relationship. There was no significant relationship between water temperature and tensile-strength loss for sampled mountain rivers but the overall relationship across all data was significant (GLM: F = 59.76, p = 8.52e-14, deviance explained = 12.8%) (all circles, black lines). A combined analysis incorporated a random effect of the two data sources. Addition of mountain river data marginally increased the regression slope estimate (-0.55) compared to Tiegs et al. (2019)[2] (-0.68) but with clear overlap shown by the confidence intervals. K_B = Boltzmann constant (0.0000862), Temp = mean river site water temperature (K), $Temp_0$ = 283.15 K. Temperatures were normalised to 10 °C[2]. Dashed lines represent 95% confidence intervals.

Tables

Supplementary Table 1: Study site information. CGC(%) represents the percentage catchment glacier cover of each river site. P = presence and A = absence of qPCR or PCR amplification of fungal ITS and the fungal *cbhI* gene. Sites marked with * hosted fungal amplification (fungal ITS, *cbhI* gene) and had upstream proglacial lakes.

Country	**Region**	**Site code**	**Latitude (°)**	**Longitude (°)**	**CGC (%)**	**Fungal ITS**	***cbhI* gene**
Austria	Eastern Alps	A1	46.83104	11.04022	64	A	A
Austria	Eastern Alps	A2	46.83633	11.03612	41	P	P
Austria	Eastern Alps	A3	46.83981	11.03206	38	P	P
Austria	Eastern Alps	A4	46.84623	11.01827	30	P	P
Austria	Eastern Alps	A5	47.12213	12.63853	36	A	A
Austria	Eastern Alps	A6	47.12403	12.63864	3	P	P
Austria	Eastern Alps	A7	47.13204	12.63389	0	P	P
Austria	Eastern Alps	A8	47.13413	12.63749	26	P	A
Austria	Eastern Alps	A9	47.14075	12.65157	46	P	P
Austria	Eastern Alps	A10	47.13359	12.63351	0	P	P
Austria	Eastern Alps	A11	47.13269	12.63310	0	P	P
Austria	Eastern Alps	A12*	47.13403	12.63727	54	P	A
Austria	Eastern Alps	A13*	47.12971	12.28085	56	P	P
Austria	Eastern Alps	A14	47.13371	12.28345	0	P	P
Ecuador	Antisana	E1	-0.46987	-78.1829	0	A	A
Ecuador	Antisana	E2	-0.49556	-78.1961	27	A	A
Ecuador	Antisana	E3	-0.50470	-78.2162	0	A	P
Ecuador	Antisana	E4	-0.51282	-78.2158	0	A	P
Ecuador	Antisana	E5	-0.51374	-78.2174	8	P	P
Ecuador	Antisana	E6	-0.47128	-81.5010	65	A	A
Ecuador	Antisana	E7	-0.45508	-81.4760	56	A	A
Ecuador	Antisana	E8	-0.46530	-78.1652	39	A	P
Ecuador	Antisana	E9	-0.50550	-78.2162	7	A	A
Ecuador	Antisana	E10	-0.51306	-78.2156	10	P	P
France	Western Alps	F1	45.296718	6.645947	51	A	A
France	Western Alps	F2	45.297519	6.650509	0	A	A
France	Western Alps	F3	45.287004	6.669283	18	A	A
France	Western Alps	F4	45.296980	6.672500	0	P	A
France	Western Alps	F5	45.305088	6.669824	10	P	P
France	Western Alps	F6	45.312892	6.681206	13	A	A
France	Western Alps	F7	45.328562	6.625382	25	A	P
France	Western Alps	F8	45.346282	6.620300	17	A	A
France	Western Alps	F9	45.346917	6.616693	0	A	A
France	Western Alps	F10	45.361999	6.585158	13	A	A
France	Western Alps	F11	45.329039	6.625382	35	P	P
New Zealand	Southern Alps	NZ1	-43.47817	170.00835	50	P	A
New Zealand	Southern Alps	NZ2	-44.47523	168.72809	0	P	A
New Zealand	Southern Alps	NZ3	-44.50284	168.72032	30	P	P
Norway	Finse	N1	60.58883	7.44862	32	A	A
Norway	Finse	N2	60.58931	7.44816	45	A	A

Norway	Finse	N3	60.57460	7.47961	85	P	A
Norway	Finse	N4	60.57524	7.48529	71	A	A
Norway	Finse	N5	60.57416	7.49403	1	A	A
Norway	Finse	N6	60.56731	7.49382	8	P	P
Norway	Finse	N7	60.56763	7.50173	80	A	P
Norway	Finse	N8	60.57802	7.50746	58	P	P
Norway	Finse	N9	60.58072	7.51330	64	A	P
Norway	Finse	N10	60.58464	7.51981	55	A	A
Norway	Finse	N11	60.58464	7.51981	53	A	A
Norway	Finse	N12	60.58880	7.44874	0	A	A
Norway	Finse	N13	60.59002	7.55209	0	A	A
Norway	Finse	N14	60.59410	7.53861	64	A	A
USA	Alaska Boundary Range	USA1	58.364416	-134.478486	26	A	A
USA	Alaska Boundary Range	USA2	58.528439	-134.805948	40	A	A
USA	Alaska Boundary Range	USA3	58.404140	-134.581596	55	A	A
USA	Alaska Boundary Range	USA4	58.652052	-134.914173	11	A	A
USA	Alaska Boundary Range	USA5	58.528330	-134.805990	44	A	A

Supplementary Table 2: GLM/GAM summary statistics. Values relate to relationships displayed in Supplementary Figure 2. Water temperature = mean river water temperature (°C), Channel stability = 1/Pfankuch Index, Turbidity = optical turbidity (NTU), *cbhI* = *cbhI* gene ln copy number/cm^2 cotton strip, ITS = fungal (ITS) ln copy number/cm^2 cotton strip, asco = Ascomycota OTU abundance, sapro = abundance of OTUs classified as hosting a saprotrophic trophic mode, *tetra* = *Tetracladium* OTU abundance and TS loss = tensile-strength loss (%) (N/DD).

Variables	**Model (Distribution)**	**χ^2 / *F***	***p*-value**	**Deviance explained (%)**
Water temperature				
cbhI	GLM (Gaussian)	4.02	0.0593	17.5
ITS	GLM (Gaussian)	6.00	0.0241	24.0
asco	GLM (Gaussian)	2.35	0.14075	10.5
sapro	GAM (Negative binomial)	173.4	< 2e-16	19.5
tetra	GAM (Negative binomial)	53.3	2.66e-12	2.48
pH				
cbhI	GLM (Gaussian)	4.59	0.0441	17.9
ITS	GAM (Gaussian)	1.243	0.313	12.8
asco	GLM (Gaussian)	0.2082	0.6524	0.9
sapro	GAM (Negative binomial)	73.9	< 2e-16	6.97
tetra	GAM (Negative binomial)	486.7	< 2e-16	25.2
TS loss	GLM (Gaussian)	11.57	< 0.0029	18.2
Channel stability				
cbhI	GAM (Gaussian)	1.30	0.302	14.8
ITS	GAM (Gaussian)	0.42	0.663	4.72
asco	GLM (Gaussian)	4.15	0.05322	15.3
sapro	GAM (Negative binomial)	39.33	2.88e-09	5.98
tetra	GAM (Negative binomial)	210.0	< 2e-16	9.36
TS loss	GLM (Gaussian)	1.46	0.2327	3.0
Turbidity				
cbhI	GAM (Gaussian)	4.91	0.0181	32.9
ITS	GLM (Gaussian)	1.66	0.212	7.3
asco	GAM (Negative binomial)	11.94	0.00256	10.3
sapro	GAM (Negative binomial)	18.15	0.00114	2.9
tetra	GAM (Negative binomial)	263.9	< 2e-16	9.6
TS loss	GLM (Gaussian)	0.005	0.946	8.8

Supplementary Table 3: Fungal responses to reducing catchment glacier cover and tensile-strength loss. Wald statistics illustrating fungal (ITS) OTUs whose relative abundance was associated significantly (Pr(>wald) = < 0.05) with either catchment glacier cover (%CGC) or tensile-strength loss (TS loss). Values were calculated with *manyglm* analysis using the *mvabund* package of R[3]. The +/- signs indicate if relative OTU abundance increased or decreased with reductions in catchment glacier cover and tensile-strength loss across the six glacierised mountain regions.

OTU Identification	Wald value	Pr(>wald)	%CGC	TS loss
Fungi (ITS)				
Lemonniera centrosphaera	110.28	0.002	+	
Tetracladium sp.	38.22	0.010	+	
Unclassified	30.84	0.031	-	
Unclassified	40.89	0.003	-	
Unclassified	45.21	0.002	-	
Helotiales sp.	50.27	0.002	+	
Unclassified	50.25	0.002	-	
Unclassified	29.70	0.045	-	
Unidentified	36.95	0.013	-	
Tetracladium marchalianum	61.52	0.002	+	
Unclassified	90.67	0.002	-	
Unclassified	31.57	0.025	-	
Leotiomycetes sp.	116.81	0.002	-	
Unclassified	31.81	0.024	-	
Tetracladium sp.	37.97	0.011	+	
Ascomycota sp.	74.88	0.002	-	
Tetracladium sp.	32.36	0.023	+	
Ascomycota sp.	54.43	0.002	+	
Tetracladium psychrophilum	94.84	0.045		-

Supplementary Table 4: Latitudinal position was not associated with changes in aquatic cellulose-decomposition rates. GLMM and GAMM summary statistics for fixed effect models (Figure 1 and Supplementary Figure 1). %CGC = catchment glacier cover (%), TS loss = tensile-strength loss (%) (N/DD), ITS = fungal (ITS) ln copy number/cm^2 cotton strip, *cbhI* = *cbhI* gene ln copy number/cm^2 cotton strip, asco = Ascomycota OTU abundance, *tetra* = *Tetracladium* OTU abundance, sapro = saprotroph OTU abundance. Addition of absolute latitude did not improve model performance (higher AIC values) for all measured relationships.

	Value	**SE**	***t***	***p*-value**	***R*²/Deviance explained (%)**	**AIC**
GLMM						
ITS vs %CGC	-0.05	0.02	-2.83	0.0101	0.24	105.22
TS loss vs ITS	0.02	0.01	2.56	0.0193	0.22	-35.93
TS loss vs *cbhI*	0.04	0.01	4.73	< 0.000147	0.52	-44.73
GAMM						
asco vs %CGC	-48.66	19.52	-2.49	0.0203	21.3	468.35
tetra vs %CGC	-16.99	14.38	-1.81	0.24946	5.7	454.07
sapro vs %CGC	-67.12	24.80	-2.71	0.0126	24.2	480.32
cbhI vs %CGC	-0.05	0.01	-3.45	0.00243	36.1	92.00

Supplementary references

1. Pfankuch, D. J. *Stream Reach Inventory and Channel Stability Evaluation* (Northern Region, Montana, US Department Forest Service, 1975).

2. Tiegs, S. D. et al.. Global patterns and drivers of ecosystem functioning in rivers and riparian zones. *Science Advances* **5,** (2019).

3. Wang, Y., Maumann, U., Wright, S. & Warton, D. *Mvabund: Statistical methods for analysing multivariate abundance data.* [Online]. [Accessed 2 November 2018]. Available from: https://cran.r-project.org/package=mvabund (2018).